Path Planning for Underactuated Dubins Micro-robots Using Switching Control*

Yatong An[1], Chao Xu[1], Qun Lin[2], Ryan Loxton[2] and Kok Lay Teo[2]

***Abstract*— In this paper, we develop an optimal path planning strategy for under-actuated Dubins micro-robots. Such robots are non-holonomic robots constrained to move along circular paths of fixed curvature clockwise or counter-clockwise. Our objective is to investigate the coverage and optimal path problems, as well as multi-robot cooperation, for a switching control scheme. Our methods are based on elementary geometry and optimal control techniques. The results in this paper show that the trajectories of micro-robots can cover the entire two-dimensional plane, and that the proposed switching control scheme allows multiple robots to cooperate. In addition, we deduce the minimum-time path under the switching control scheme by converting the robot model into the traditional Dubins vehicle model.**

I. INTRODUCTION

Power supply for micro-robots is a challenging topic and a major obstacle to creating functional micro-robots. To solve the power supply problem, researchers have proposed several different solutions. One approach is to use on-board power supplies, such as power generators based on micro-electromechanical systems (MEMS) and chemical energy-based generators. Furthermore, as an alternative to carrying or producing energy on-board, micro-robots can be placed in an external field, such as a magnetic field, with the interaction between the field and the micro-robot providing the driving force [1].

The small size of micro-robots makes them difficult to power through on-board energy supplies or generators, which are very complex and expensive to produce at the microscopic scale. Thus, on-board energy and propulsion systems still have many obstacles and a long way to go. Consequently, inspired by maglev technology [2] and magnetic resonance imaging (MRI) [3], the idea of using a magnetic field to actuate micro-robots has received more and more attention. It is well-known that in high-energy physics, energy is not continuous and only quantized energy is available at the microscopic level. At the same time, it is much easier to design discrete control decisions rather than continuous sequences, i.e., simple control language words. For these reasons, micro-robots that can only move in several distinct states have become popular. For example, in [4], an untethered, electrostatic, MEMS micro-robot has been described that has only two driving modes: translate forward, or turn through an arc with a fixed minimum radius of approximately 175 μm. Such vehicle models are known as the Dubins vehicle in the literature [5]. Here, we call such micro-robots "Dubins Micro-robots".

The Dubins micro-robot that we consider in this paper is also a type of Dubins vehicle. For simplicity, we consider a very basic but extremely important prototype of the Dubins micro-robot, where the interaction between charged particles and electromagnetic fields is used to manipulate the micro-robot. In contrast with the standard Dubins vehicle, the prototype that we consider can only move in two different states—rotate clockwise and rotate counter-clockwise—due to the simplified design of the driving system.

The main contributions of this paper are as follows. First, we propose a prototype of the Dubins micro-robot and describe its feasible path. Unlike the standard Dubins model, we do not consider straight line movement because in many cases straight line movement is difficult to control due to the electro-magnetic noises. Thus, we only consider clockwise and counter-clockwise circular paths. We call our prototype the under-actuated Dubins model. Second, we study the reachable set and introduce the so-called "coverage problem" for the Dubins micro-robot. Third, we analyze the cooperation problem for multi-robot systems, including how to design the optimal path for multiple robots to cooperate. Finally, and most importantly, we design the minimum-time path for the under-actuated Dubins model step-by-step. We successfully convert this problem into the traditional Dubins model, and then derive our conclusions using optimal control theory.

II. PROBLEM FORMULATION

In this section, we introduce the main problem of the paper and review some basic notions. The goal of the paper is to find the optimal path for a Dubins micro-robot to execute certain task, such as killing a cancer cell in magnetic chemotherapy. We will first introduce the dynamic model for the micro-robot and then discuss several fundamental issues, including the coverage problem and the cooperation problem.

A. Dubins micro-robot and its feasible path

We propose a simple prototype for the Dubins micro-robot, where the motion of the robot is powered by the interaction between charged particles and electromagnetic fields. Based

*This work was partially supported by the National Natural Science Foundation of China (F030119), the Zhejiang Provincial Natural Science Foundation (Y1110354) and the Fundamental Research Funds for Central Universities (1A5000-172210101).

[1]Y. An (ytan@zju.edu.cn) and C. Xu (cxu@zju.edu.cn) are with the Department of Control Science and Engineering, Zhejiang University, Hangzhou, 310027, China.

[2]Q. Lin (q.lin@curtin.edu.au), R. Loxton (r.loxton@curtin.edu.au) and K. L. Teo (k.l.teo@curtin.edu.au) are with the Department of Mathematics and Statistics, Curtin University, Perth, 6845, Australia.

on the Lorentz theorem for a charged particle moving in a magnetic field, the Lorentz force can be expressed as follows:

$$\mathbf{F} = q\mathbf{v} \times \mathbf{B}, \tag{1}$$

where q is the charge of the particle, $\mathbf{B}$ is the magnetic field vector and $\mathbf{v}$ is the velocity vector of the particle.

We can also derive the centrifugal force of the particle in the magnetic field:

$$\|\mathbf{F}\| = \frac{m\|\mathbf{v}\|^2}{R}, \tag{2}$$

where m is the mass of the particle and R is the radius of the circular trajectory of the particle.

Define B_x, B_y and B_z as the x-, y- and z-components of the magnetic field in the Cartesian Coordinates. If the direction of the magnetic field is perpendicular to the motion plane of the particle, then the x- and y-components of the magnetic field are zero [6], [7]. In other words, $B_x = 0$, $B_y = 0$, and $v_z = 0$. This implies

$$m\frac{\|\mathbf{v}\|^2}{R} = q\|\mathbf{v}\|\|\mathbf{B}\|. \tag{3}$$

Hence,

$$\|\mathbf{v}\| = \frac{q\|\mathbf{B}\|R}{m}. \tag{4}$$

As in Figure 1, let α denote the angle between the x-axis and the straight line passing through the origin O and the current position P. Here, counter-clockwise means the positive direction. From basic geometry, we know that

$$v_x = \|\mathbf{v}\|\sin\alpha, \quad v_y = -\|\mathbf{v}\|\cos\alpha. \tag{5}$$

Substituting equation (4) into equation (5) gives

$$\dot{x} = \frac{q\|\mathbf{B}\|R}{m}\sin\alpha, \ \dot{y} = -\frac{q\|\mathbf{B}\|R}{m}\cos\alpha, \tag{6}$$

where (x, y) is the position of the particle in the motion plane. Also, the rate of change in the angle α is

$$\dot{\alpha} = \frac{qB_z}{m}. \tag{7}$$

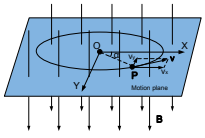

Fig. 1. System model.

We adopt a hybrid control scheme in which the control consists of discrete values. Here, the direction of the magnetic field is the manipulated variable. Thus, $B_z = \|\mathbf{B}\|$ or $B_z = -\|\mathbf{B}\|$. It follows that we can rewrite (6),(7) in the following form:

$$\dot{x} = C\sin\alpha, \ \dot{y} \ = -C\cos\alpha, \ \dot{\alpha} = u, \tag{8}$$

where $C = \frac{q\|\mathbf{B}\|R}{m}$ and $u = \frac{qB_z}{m}$.

It is clear from (8) that the feasible path for the micro-robot is either a clockwise or counter-clockwise circle. Note that, in contrast with the traditional Dubins vehicle [5], the micro-robot considered here cannot move in a straight line—only in clockwise or counter-clockwise circles.

B. The coverage problem and switching control scheme

The micro-robot dynamics exhibit different modes of evolution, with each mode characterized by different dynamic features. Systems of this type are called switched systems [8]. A switched system can be modeled by assigning:

- A family $\mathcal{F} = \{f_n\}_{n\in\mathcal{N}}$ of smooth vector fields $f_n : \mathbf{R}^d \to \mathbf{R}^d$, where f_n defines the dynamic behaviour of the nth mode, d is the dimension of the state space, and $\mathcal{N}$ is a given set of indices;
- A rule that determines the switching policy, i.e., when the system should switch from one mode to another.

The switching rule is completely specified by a sequence of switching times $\{t_i\}$ and a sequence of indices $\{n_i\}$, where n_i denotes the index of the active vector field (or mode) on the interval $[t_i, t_{i+1})$. Figure 2 illustrates the switched system model for the Dubins micro-robot, where the switching mechanism is caused by the change in direction of the magnetic field. As shown in Figure 2, the guard and reset conditions correspond to the switching times. That is, the switching times determine when the robot should change from one mode to another.

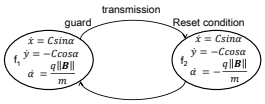

Fig. 2. Switched system model.

Let D denote the desired point in the motion plane (arbitrarily chosen). Furthermore, let X denote the continuous state space of the micro-robot and let X_0 denote the initial state. Then, the coverage problem is to consider whether the arbitrary point D can be reached by the robot. If this is true, then how can one determine the switching times $\{t_i\}$, given the initial state X_0.

C. Multi-robot cooperation

In this part, we will consider the cooperation of multiple Dubins micro-robots. The problem that we consider is whether two micro-robots can meet (i.e., their states should coincide at a certain time) starting from two arbitrary initial states. Recall that the only control variable is the direction of the magnetic field (this causes the switching mechanism). The micro-robots are controlled by the same magnetic field, which means that the dynamic behaviour of each micro-robot is the same at any time. The problem is to determine a set of switching times $\{t_i\}$ such that the states of the two micro-robots X_{p_1} and X_{p_2} are equal at a specific terminal time T, i.e., $X_{p_1}(T) = X_{p_2}(T)$. See Figure 3.

D. Minimum-time switching control

The problem we consider here is to find the minimum-time path for the micro-robot to arrive at the desired point from

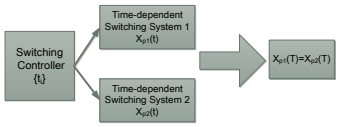

Fig. 3. Multi-robot cooperation task.

a specified initial point. For this problem, the existing path planning methods mentioned above are inappropriate for the dynamic model of the Dubins micro-robot. We formulate the minimum-time problem as follows:

$$\min \quad J = T = \int_0^T 1dt \tag{9}$$

subject to the (re-scaled) dynamics

$$\begin{cases} \dot{x} = R\sin\alpha, \\ \dot{y} = -R\cos\alpha, \\ \dot{\alpha} = u, \end{cases} \tag{10}$$

the constraints

$$u \in \{1, -1\},\ X(0) = X_0,\ X(T) = X_f, \tag{11}$$

where X_0 denotes the given initial position and X_f denotes the desired final position. This problem is difficult because the input constraints are discrete. Thus, the problem is actually an optimal discrete-valued control problem [9]. In the next section, we will discuss an analytical solution to this problem.

III. Switching Control Scheme

In this section, we investigate switching control strategies for the problems described in Section II: the single robot coverage problem, the multi-robot cooperation problem, and the minimum-time switching control problem.

A. The coverage problem

(1) Here, our goal is to determine whether the set of possible robot states X can cover the entire motion plane. If this is true, then a further objective is to determine appropriate switching times $\{t_i\}$ for moving the robot from any initial state X_0 to any final state X_f, given the dynamic equations for the robot's motion.

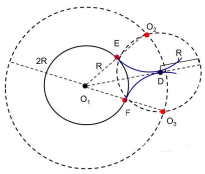

Fig. 4. Diagram for the coverage proof.

As can be seen in Figure 4, O_1 is the center of the initial circular trajectory, and D is the desired terminal point, which is arbitrarily chosen such that its distance from O_1 is between R and $2R$. It is obvious that the distance between the desired point D and the center of the circle on which D lies should be R. Furthermore, the distance between O_1 and the center of the circle on which D lies should be $2R$ because the circle containing D is tangent to the original circle. We can draw a circle of radius R centered at D; see Figure 4. We draw another circle of radius $2R$ centered at O_1. The points of intersection of these circles, denoted by O_2 and O_3, should be the center of the desired circle on which D lies. The line from O_1 to O_2 will intersect the circle centered at O_1 at the point E, which is the switching point.

So far, we have proved that the circular ring area of radius between R and $2R$ centered at O_1 can be reached if we choose the appropriate switching point. Performing this switching, and then applying a similar argument with the new circle as the initial circle, we can reach any point in the 2-dimensional plane, i.e., planar controllability.

(2) In this part, we are only concerned with feasible switching control schemes that deliver the particle to the desired point, irrespective of optimality. The goal is to design the switching control scheme to control the particle to arrive at the desired point.

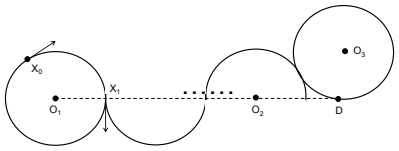

Fig. 5. Motion of the particle under a switching control scheme.

From Figure 5, suppose that we want the particle to arrive at point D from its current position X_0. Let O_1 denote the center of the circle for the current portion of the particle's trajectory. If we are not concerned with optimality, then it is easy to find a feasible trajectory delivering the particle to point D. We first draw a straight line connecting O_1 and D, denoted by l_{O_1D}. Once the particle reaches the line l_{O_1D}, it can move along a series of semi-circles until arriving at the circle centered at O_2 (the last circle before D). Draw a circle containing D that is tangent to the circle centered at O_2. The intersection of the two circles is the final switching point.

B. Multi-robot cooperation

From Figure 6, we assume that two particles P_1 and P_2 are in the same magnetic field. We know that the trajectories of P_1 and P_2 will have the same dynamic behaviour because their motions are controlled by the same switching magnetic field. Furthermore, we can ensure that the collision point is on the line perpendicular to the line between P_1 and P_2 (denoted by $l_{P_1P_2}$) and passing through the mid-point of $l_{P_1P_2}$. This line is called the mid-perpendicular.

We choose any point on the mid-perpendicular line and denote this point by D. From the results in Section III-A, we know that there exists trajectories leading each particle to D. If we rotate point P_1 around point D (represented by the dotted curve), then P_1 will eventually reach P_2, and the trajectory will coincide with the trajectory starting at P_2.

From Figure 6, h is the distance between the convergence point (denoted by D) and the mid-point of the line between P_1 and P_2 (denoted by P_M). Draw a circle around D and its radius is h. Draw another line which is tangent to circle D and pass through point P_2, and the point of tangency is denoted by P_N. Furthermore, β is the angle between $l_{P_1P_2}$ and $l_{P_2P_N}$, as shown in Figure 6. From the discussion above, when D changes, β will also change. It is clear that when $\beta = 0$, the two particles will never meet. However, when $\beta \neq 0$, the two particles can meet. The relationship between β and h is given by:

$$\beta = \pi - 2\arctan\frac{h}{l_{P_2P_N}}, \tag{12}$$

where $P_2P_N = P_2P_M$.

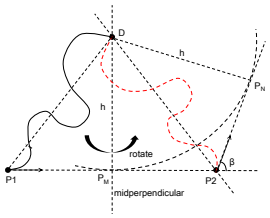

Fig. 6. Analysis of two particles converging.

C. Minimum-time switching control

As discussed in Section II-D, the minimum-time switching control problem can be formulated as shown in equations (9)-(11). Dubins studied a similar problem using differential geometry [5]. However, in our problem, unlike in the traditional Dubins problem, the micro-robot cannot move in a straight line.

We first try to convert this problem into the traditional Dubins model. From equation (10), we obtain

$$\dot{x}^2 + \dot{y}^2 = \text{constant}, \tag{13}$$

which means that the velocity of the particle is constant. Also, we know that the angle α in Figure 7 is proportional to the time t. Hence, finding the minimum-time path is equivalent to finding the shortest path.

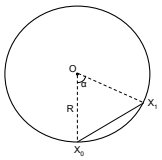

Fig. 7. Diagram for the minimum-time proof.

Also, because the speed is fixed, in a circle, the central angle α is proportional to the time. So, finding the longest distance in unit time is equivalent to finding the longest distance in unit angle. This can be solved by finding the maximum value of the first derivative:

$$\frac{dl_{X_0X_1}}{d\alpha} = \frac{d(2R\sin\frac{\alpha}{2})}{d\alpha} = R\cos\frac{\alpha}{2}, \tag{14}$$

where $l_{X_0X_1}$ represents the linear distance between X_0 and X_1. It is clear that $\frac{dl_{X_0X_1}}{d\alpha} \to R$ as $\alpha \to 0$, which is the maximum value. Consequently, we know that if we switch the direction of the magnetic field more frequently, then the longer the displacement is in unit time. If the switching duration can tend to 0, then the curve can tend to a straight line. Thus, this problem is converted into the traditional Dubins model.

Now, consider this Dubins problem, which is the same as the problem in literature [10].

$$\begin{aligned} \min \quad & J = T = \int_0^T 1dt, \\ \text{s.t.} \quad & \begin{cases} \dot{x} = R\sin\alpha, \\ \dot{y} = -R\cos\alpha, \\ \dot{\alpha} = u, \end{cases} \\ \text{where} \quad & \|u\| \leq 1,\ X(0) = X_0,\ X(T) = X_f. \end{aligned}$$

From the conclusions in literature [10], the optimal path can only have the following forms:

- concatenation of a bang-bang piece (arc of a circle, $u = \pm 1$), a singular piece (segment of a line, $u = 0$), and a bang-bang piece.
- concatenation of bang-bang pieces with no more than 3 switchings, the arcs of circles between switchings having the same central angle $\in [\pi, 2\pi)$.

Then, let us come back to the original problem. If the incidence angle is not specific, then the optimal path is also the concatenation of a bang-bang control piece and a singular piece, such as the following forms in Figure 8.

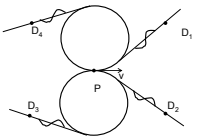

Fig. 8. Optimal Path.

Notice that the straight line are the approximation of frequent switching arcs, and the end point can be guaranteed to be arrived at by the conclusions in part III-A.

IV. Numerical Computation

Having analyzed the switching control scheme from a theoretical viewpoint in the previous section, we now want to compute the optimal switching times for the switching control scheme. It is well-known in optimal control that standard optimization algorithms do not perform adequately when used to optimize variable switching times (see [11]). Thus, we will use the time-scaling transformation described in [12], [11] to transform the variable switching times to fixed points in a new time horizon. This yields an equivalent optimization problem in which the switching times are fixed. This equivalent problem can then be solved using a standard gradient-based optimization algorithm (such as sequential quadratic programming) in conjunction with the gradient computation scheme described in [12].

A. Minimum-time switching control: Single robot

Consider the problem of minimizing the time taken for the robot to travel from (x_0, y_0) to (x_f, y_f). The problem is:

$$\begin{aligned} \min \quad & T \\ \text{s.t.} \quad & \dot{x} = R\sin\alpha,\ \dot{y} = -R\cos\alpha,\ \dot{\alpha} = u, \\ & (x(0), y(0)) = (x_0, y_0), \\ & (x(T), y(T)) = (x_f, y_f), \\ & u \in \{-1, +1\}. \end{aligned}$$

Let p be an integer such that $2p-1$ is an upper bound for the number of times that the magnetic field switches direction. Then, the dynamics for the micro-robot can be expressed as the following switched system:

$$\left.\begin{aligned} \dot{x} &= R\sin\alpha, \\ \dot{y} &= -R\cos\alpha, \\ \dot{\alpha} &= 1, \end{aligned}\right\} \quad t \in [t_{2i}, t_{2i+1}), \quad i = 0, \ldots, p-1,$$

and

$$\left.\begin{aligned} \dot{x} &= R\sin\alpha, \\ \dot{y} &= -R\cos\alpha, \\ \dot{\alpha} &= -1, \end{aligned}\right\} \quad t \in [t_{2i-1}, t_{2i}), \quad i = 1, \ldots, p.$$

Note that if less than $2p-1$ switches are required, then we will have $t_i = t_{i+1}$ for some indices i (i.e., some of the switching times will coincide). The problem that we face is to choose the switching times $\{t_i\}$ so that the final time T is minimized. Switching time optimization problems such as this pose difficulties for standard gradient-based optimization methods. Thus, we will apply the time-scaling transformation.

In the time-scaling transformation, we introduce a new time variable $s \in [0, 2p]$ and relate s to t through the following differential equation:

$$\frac{dt(s)}{ds} = \theta_i, \quad s \in [i-1, i), \quad i = 1, \ldots, 2p, \tag{15}$$

$$t(0) = 0, \tag{16}$$

$$t(2p) = T, \tag{17}$$

where $\theta_i = t_i - t_{i-1}$ is the duration between the ith and $(i-1)$th switching times in the original time horizon. Clearly,

$$\theta_i \geq 0, \quad i = 1, \ldots, 2p.$$

By integrating (15)-(17), it is easy to see that $t = t(s)$ is a piecewise-linear function of the new time variable s. In particular,

$$t(i) = \theta_1 + \theta_2 + \cdots + \theta_i = t_i, \quad i = 0, \ldots, 2p.$$

This shows that $s = i$ is mapped to $t = t_i$ under the time-scaling transformation defined by (15)-(17). Applying (15)-(17) to the switched system describing the motion of the micro-robot, we obtain

$$\left.\begin{aligned} \dot{x} &= \theta_i R\sin\alpha, \\ \dot{y} &= -\theta_i R\cos\alpha, \\ \dot{\alpha} &= \theta_i, \end{aligned}\right\} \quad s \in [2i, 2i+1), \quad i = 0, \ldots, p-1,$$

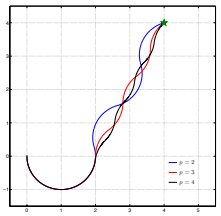

Fig. 9. Optimal path for the minimum-time problem in Section IV-A.

and

$$\left.\begin{aligned} \dot{x} &= \theta_i R\sin\alpha, \\ \dot{y} &= -\theta_i R\cos\alpha, \\ \dot{\alpha} &= -\theta_i, \end{aligned}\right\} \quad s \in [2i-1, 2i), \quad i = 1, \ldots, p.$$

The boundary conditions become

$$(x(0), y(0)) = (x_0, y_0), \quad (x(2p), y(2p)) = (x_f, y_f).$$

The problem is to choose the durations $\{\theta_i\}$ to minimize $T = \theta_1 + \cdots + \theta_{2p}$. This problem is a switched system optimal control problem in which the switching times are fixed. The only decision variables are the durations $\{\theta_i\}$. To solve this problem, we can view it as a nonlinear optimization problem in which the decision variables are $\{\theta_i\}$ and there are two constraints: $x(2p) = x_f$ and $y(2p) = y_f$. Note that the state trajectory of the robot is completely determined by $\{\theta_i\}$. Thus, the objective and constraints are completely determined by $\{\theta_i\}$. To solve the minimum-time problem as a nonlinear optimization problem, we need to determine the gradient of $T = \theta_1 + \cdots + \theta_{2p}$ and the gradient of the constraints $x(2p) = x_f$ and $y(2p) = y_f$ with respect to $\{\theta_i\}$. The gradient of the objective is straightforward because it is an explicit function of $\{\theta_i\}$. The gradient of the terminal constraints is not straightforward because $\{\theta_i\}$ influences the constraints implicitly through the dynamic system. Nevertheless, the constraint gradients can be computed using the algorithm described in [12].

As an example, let $(x_0, y_0) = (0, 0)$ and $(x_f, y_f) = (4, 4)$. We wrote a Fortran program to solve the minimum-time problem (post time-scaling transformation). This program combines the optimization software NLPQLP [13] with the gradient computation algorithm in [12]. We choose $R = 1$. We solved the problem for $p = 2, 3, 4$, giving optimal terminal times of $T = 8.14$, $T = 7.78$, and $T = 7.69$, respectively. The optimal durations for $p = 2$ are

$$\theta_1 = 3.43,\ \theta_2 = \theta_3 = \theta_4 = 1.57.$$

The optimal durations for $p = 3$ are

$$\theta_1 = 3.14,\ \theta_2 = \theta_3 = \theta_4 = \theta_5 = \theta_6 = 0.93.$$

The optimal durations for $p = 4$ are

$$\theta_1 = 3.02,\ \theta_2 = \theta_3 = \theta_4 = \theta_5 = \theta_6 = \theta_7 = \theta_8 = 0.67.$$

The optimal robot trajectories for $p = 2, 3, 4$ are shown in Figure 9.

B. Cooperation problem: Two robots

In this case, we have two dynamic systems—one for each micro-robot. Let (x_1, y_1) denote the position of the first micro-robot and let (x_2, y_2) denote the position of the second micro-robot. Then

$$\left.\begin{aligned} \dot{x}_j &= R\sin\alpha_j, \\ \dot{y}_j &= -R\cos\alpha_j, \\ \dot{\alpha}_j &= 1, \end{aligned}\right\} \quad t \in [t_{2i}, t_{2i+1}), \quad i = 0, \ldots, p-1,$$

and

$$\left.\begin{aligned} \dot{x}_j &= R\sin\alpha_j, \\ \dot{y}_j &= -R\cos\alpha_j, \\ \dot{\alpha}_j &= -1, \end{aligned}\right\} \quad t \in [t_{2i-1}, t_{2i}), \quad i = 1, \ldots, p,$$

where $j \in \{1, 2\}$ and p is as defined in Section IV-A. The initial conditions are

$$(x_1(0), y_1(0)) = (x_{10}, y_{10}), \quad (x_2(0), y_2(0)) = (x_{20}, y_{20}).$$

Since we require the micro-robots to converge to the same location, the terminal conditions are

$$x_1(T) = x_2(T), \quad y_1(T) = y_2(T).$$

Applying the time-scaling transformation (15)-(17) yields

$$\left.\begin{aligned} \dot{x}_j &= \theta_i R\sin\alpha_j, \\ \dot{y}_j &= -\theta_i R\cos\alpha_j, \\ \dot{\alpha}_j &= \theta_i, \end{aligned}\right\} \; s \in [2i, 2i+1), \; i = 0, \ldots, p-1,$$

and

$$\left.\begin{aligned} \dot{x}_j &= \theta_i R\sin\alpha_j, \\ \dot{y}_j &= -\theta_i R\cos\alpha_j, \\ \dot{\alpha}_j &= -\theta_i, \end{aligned}\right\} \; s \in [2i-1, 2i), \; i = 1, \ldots, p,$$

where $j \in \{1, 2\}$. The terminal constraint becomes

$$x_1(2p) = x_2(2p), \quad y_1(2p) = y_2(2p). \tag{18}$$

The problem is to choose $\{\theta_i\}$ to minimize $T = \theta_1 + \cdots + \theta_{2p}$ subject to constraints (18). This problem can be solved in a similar way to the single-robot problem in Section IV-A, i.e., by combining the gradient computation algorithm in [12] with a nonlinear optimization method such as sequential quadratic programming.

As an example, let $(x_{10}, y_{10}) = (0, 0)$, $(x_{20}, y_{20}) = (7, 0)$. The initial angle for the first robot is $\alpha_1(0) = 0$ and the initial angle for the second robot is $\alpha_2(0) = \pi/3$. We choose $R = 1$. Solving the problem for $p = 2, 3, 4$ gives optimal terminal times of $T = 11.27$, $T = 9.84$, and $T = 9.61$, respectively. The optimal durations for $p = 2$ are

$$\theta_1 = 4.01, \; \theta_2 = \theta_3 = \theta_4 = 2.42.$$

The optimal durations for $p = 3$ are

$$\theta_1 = 3.51, \; \theta_2 = \theta_3 = \theta_4 = \theta_5 = \theta_6 = 1.27.$$

The optimal durations for $p = 4$ are

$$\theta_1 = 3.34, \; \theta_2 = \theta_3 = \theta_4 = \theta_5 = \theta_6 = \theta_7 = \theta_8 = 0.90.$$

The optimal trajectories are shown in Figure 10.

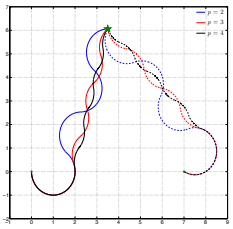

Fig. 10. Optimal path for the minimum-time problem in Section IV-B.

V. Conclusions

In this paper, we introduced the under-actuated Dubins micro-robot whose motion is based on the interaction between charged particles and an external magnetic field. We described the dynamic model for the Dubins micro-robot and its feasible path. The micro-robot is controlled via a switching control scheme, where the switching mechanism is invoked by changing the direction of the magnetic field. We studied the coverage problem and the cooperation problem for multiple robots. We also showed that these problems can be solved numerically using the time-scaling transformation.

References

[1] M. Mehrtash, N. Tsuda, and M. B. Khamesee, "Bilateral macroCmicro teleoperation using magnetic levitation," *IEEE-ASME Transactions on Mechatronics*, vol. 16, pp. 459–469, 2011.

[2] H.-W. Lee, K.-C. Kim, and J. Lee, "Review of maglev train technologies," *IEEE Transactions on Magnetics*, vol. 42, pp. 1917–1925, 2006.

[3] D. Folio, C. Dahmen, T. Wortmann, M. A. Zeeshan, K. Shou, S. Pane, B. J. Nelson, A. Ferreira, and S. Fatikow, "MRI magnetic signature imaging, tracking and navigation for targeted micro/nano-capsule therapeutics," in *International Conference on Intelligent RObots and Systems - IROS*, pp. 1297–1303, 2011.

[4] B. R. Donald, C. G. Levey, C. D. McGray, I. Paprotny, and D. Rus, "An untethered, electrostatic, globally controllable MEMS micro-robot," *IEEE/ASME Journal of Microelectromechanical Systems*, vol. 15, pp. 1–15, 2006.

[5] L. E. Dubins, "On curves of minimal length with a con-straint on average curvature and with prescribed initial and terminal positions and tangents," 1957.

[6] J. Lee, R. Post, and H. Ishii, "ZeroN: mid-air tangible interaction enabled by computer controlled magnetic levitation," pp. 327–336, 2011.

[7] S. Hosseini, M. Mehrtash, and M. B. Khamesee, "Design, fabrication and control of a magnetic capsule-robot for the human esophagus," *Microsystem Technologies-micro-and Nanosystems-information Storage and Processing Systems*, vol. 17, pp. 1145–1152, 2011.

[8] D. Liberzon, *Switching in systems and control*. Boston:Birkhauser Inc, 2003.

[9] C. Yu, B. Li, R. Loxton, and K. L. Teo, "Optimal discrete-valued control computation," *Journal of Global Optimization*, 2013, to appear.

[10] A. A. Agrachev and Y. L. Sachkov, *Control theory from the geometric viewpoint*. Springer-verlag Berlin Heidelberg New York, 2004.

[11] Q. Lin, R. C. Loxton, K. L. Teo, and Y. Wu, "Optimal control computation for nonlinear systems with state-dependent stopping criteria," *Automatic*, vol. 48, pp. 2116–2129, 2012.

[12] Q. Lin, R. Loxton, K. L. Teo, and Y. H. Wu, "A new computational method for optimizing nonlinear impulsive systems," *Dynamics of Continuous, Discrete, and Impulsive Systems – Series B: Applications and Algorithms*, vol. 18, pp. 59–76, 2011.

[13] K. Schittkowski, *NLPQLP: A Fortran implementation of a sequential quadratic programming algorithm with distributed and non-monotone line search - User's guide, version 2.24*. University of Bayreuth, Bayreuth, June 2007.